Relativistic density functional theory modeling of plutonium and americium higher oxide molecules

Andréi Zaitsevskii, Nikolai S. Mosyagin, Anatoly V. Titov, and Yuri M. Kiselev

Citation: J. Chem. Phys. **139**, 034307 (2013); doi: 10.1063/1.4813284
View online: http://dx.doi.org/10.1063/1.4813284
View Table of Contents: http://jcp.aip.org/resource/1/JCPSA6/v139/i3
Published by the AIP Publishing LLC.

Relativistic density functional theory modeling of plutonium and americium higher oxide molecules

Andréi Zaitsevskii,[1,2,a] Nikolai S. Mosyagin,[2,3] Anatoly V. Titov,[2,3] and Yuri M. Kiselev[4]
[1]*NRC "Kurchatov Institute", 1 Kurchatov sq., Moscow 123182, Russia*
[2]*Petersburg Nuclear Physics Institute, Gatchina, St.-Petersburg District 188300, Russia*
[3]*Department of Physics, St.-Petersburg State University, St.-Petersburg 198904, Russia*
[4]*Department of Chemistry, M. Lomonosov Moscow State University, Vorob'evy gory, Moscow 119899, Russia*

(Received 16 April 2013; accepted 24 June 2013; published online 17 July 2013)

The results of electronic structure modeling of plutonium and americium higher oxide molecules (actinide oxidation states VI through VIII) by two-component relativistic density functional theory are presented. Ground-state equilibrium molecular structures, main features of charge distributions, and energetics of AnO_3, AnO_4, An_2O_n (An=Pu, Am), and $PuAmO_n$, $n = 6$–8, are determined. In all cases, molecular geometries of americium and mixed plutonium–americium oxides are similar to those of the corresponding plutonium compounds, though chemical bonding in americium oxides is markedly weaker. Relatively high stability of the mixed heptoxide $PuAmO_7$ is noticed; the Pu(VIII) and especially Am(VIII) oxides are expected to be unstable. © *2013 AIP Publishing LLC*. [http://dx.doi.org/10.1063/1.4813284]

I. INTRODUCTION

The discovery of Pu(VII) compounds in 1967 was followed by numerous unsuccessful attempts to find the Pu(VIII) oxide in volatile products of the oxidation of Pu(VII)-containing substances (see Refs. 1 and 2 for early reviews). In 2002, three kinds of highly volatile species interpreted as binary oxides were observed in thermochromatographic experiment with ultramicroamounts of Pu compounds;[3,4] it was suggested that one of them could be PuO_4. However, the conclusions about the molecular composition in the cited works were based mainly on arguments from analogy, and the probability of errors was rather high. The formation of volatile PuO_4 was not confirmed in similar independent experiment.[5] No Pu(VIII) compounds were detected in Pu(VI) ozonation products by X-ray photoelectron spectroscopy.[6]

In 2011,[7] the volatilization of plutonium compounds in the process of ozonation of alkaline solutions of macroamounts of Pu(VI) hydroxo complexes within the temperature range 60-90 °C was observed by α-spectrometry. The volatile compound was presumably identified as the plutonium tetroxide. This hypothesis is indirectly supported by the fact that the lower neutral plutonium oxides are insoluble in aqueous and non-aqueous media and significantly evaporate only above their melting points, i.e., at the temperatures exceeding 1000 °C,[8] so that the plutonium oxide, volatile at low temperatures, would be its higher oxide. Another argument of the authors of Ref. 7 in favor of this assignment was based on the similarity to the behavior of other highly volatile and easily sublimable M(VIII) compounds such as OsO_4 and RuO_4. Very recently, a pronounced (several orders of magnitude) enhancement of volatilization of an americium compound (probably its higher oxide) from alkaline solutions under ozonation due to the presence of plutonium has been reported.[9] This result encourages theoretical studies of americium and mixed Pu–Am higher oxide molecules.

The information on higher oxide molecules of Pu and especially Am obtained from first principle based electronic structure calculations is rather fragmentary. Fully relativistic *ab initio* and density functional theory (DFT) studies on the ground electronic state of PuO_3 and PuO_4 molecules have been reported in Ref. 10. Scalar relativistic DFT electronic structure modeling of hypothetical tetrahedral isomer of PuO_4 has been described in Ref. 11. A recent relativistic DFT study on plutonium higher oxide molecules[12] has predicted a remarkable stability of the Pu(VII) oxide molecule, Pu_2O_7; according to the results of this work, PuO_3 and PuO_4 should be markedly less stable. The positions of the two Pu atoms in the equilibrium configuration of Pu_2O_7 are not equivalent. Though their net charges are nearly equal, structure features allow to discern PuO_4-like and PuO_3-like fragments of the Pu_2O_7 molecule. One can suppose that the replacement of Pu in the latter fragment by Am could yield rather stable mixed plutonium–americium heptoxide molecule; its formation could explain the americium volatilization enhancement in the presence of Pu.[9]

The present work reports the results of relativistic DFT (RDFT) calculations for the structures and energetic properties of plutonium, americium, and mixed higher oxide molecules in their ground electronic states, which should give insight into the gas phase thermodynamics of these compounds and possible composition of volatile products of oxidation (especially ozonation) of Pu and Am compounds. Note that we use conventional formal definition of oxidation state

[a]Electronic mail: azaitsevskii@pnpi.spb.ru. URL: http://www.qchem.pnpi.spb.ru

which obviously does not reflect particular features of chemical bonding.

II. COMPUTATIONAL DETAILS

The relativistic electronic structure model employed in the present work was defined by accurate shape-consistent semilocal two-component pseudopotentials[13,14] replacing the 60-electron cores of Pu and Am. These pseudopotentials were derived from outer (valence) shell solutions of the atomic Dirac–Fock–Breit equations with the Fermi nuclear model. The optimal description of the valence (rather than semicore) shells appears essential for reproducing the chemical properties of actinides.[13] The molecular semicore/valence many-electron problem was solved by the two-component non-collinear relativistic DFT technique[15,16] with the fully unrestricted optimization of Kohn–Sham one-electron spinors. We used weakly contracted (10*s*9*p*8*d*6*f*2*g*)/[8*s*8*p*6*d*5*f*2*g*] Gaussian basis sets for actinide atoms.[17] All relatively compact basis functions were optimized in spin–orbit-coupled atomic calculations while the exponential parameters of the most diffuse *spd* and all *g* primitive Gaussians were taken from Refs. 18–20, respectively. Oxygen-centered basis sets [6*s*4*p*2*d*] were obtained by augmenting the triple zeta basis from Ref. 21 by diffuse functions. The results were quite stable with respect to the further extension of the bases; the smallness of basis set superposition errors estimated for diatomics by the Boys–Bernardi scheme (∼1 kJ/mol) eliminates the need to use any counterpoise corrections. Two approximations for the exchange-correlation functional were used throughout: the PBE0 hybrid functional[22] has been chosen because of its (partially) non-empirical nature, whereas the choice of the famous B3LYP protocol[23] was based on the results of earlier numerical experiments concerning actinide oxides.[24] The ground-state character of the obtained solutions of Kohn–Sham equations was carefully checked by swapping higher occupied and lower virtual orbitals and repeating the iterative procedure. Stationary points of the potential hypersurfaces were searched by a gradient minimization procedure using a large variety of non-symmetrical starting geometries compatible with typical An–O bond lengths. Geometries with short O–O distances were excluded in order to prevent convergence to peroxide-like structures which are out of scope of the present study; the only exception was made for AnO_4 systems where the formally octavalent structures seem unstable. The nature of the located stationary points was determined through computing the Hessian matrices by numerical differentiation of analytical energy gradients. These matrices were also used to compute the zero-point energies and thermal contributions to the gas-phase reaction enthalpies within the harmonic normal mode/rigid rotor approximation using the Firefly quantum chemistry code.[25] The reliability of the employed computational scheme is confirmed by the results of bond energy calculations for the lower oxides (Table I). Note that our estimates seem to agree better with the experimental data than those of the recent DFT study.[26]

TABLE I. Bond dissociation enthalpies of Pu and Am oxides, $\Delta H^0_{298}(AnO_n \rightarrow AnO_{n-1} + O)$, in kJ/mol.

	RDFT/PBE0[a]	RDFT/B3LYP[a]	RDFT[b]	CCSD(T)[c]	Exptl.[d]
PuO	656	639	604		658 ± 10
PuO_2	596	594	580	602	599 ± 22
PuO_3	379	387			
PuO_4	262	262			
AmO	551	539	498		582 ± 34
AmO_2	503	490	478	460	509 ± 65
AmO_3	300	306			
AmO_4	204	214			

[a]Present work.
[b]Reference 26.
[c]Reference 24, bond energies from all-electron scalar relativistic coupled-cluster calculations involving singles, doubles, and perturbative triples, corrected for spin–orbit couplings.
[d]Reference 29.

Bader analysis of charge densities was performed with the code described in Refs. 27 and 28.

III. RESULTS AND DISCUSSION

The main results concerning the equilibrium structures and energetic properties of Pu and Am higher oxide molecules are collected in Tables I–III. Along with reaction enthalpies, we also list the computed values of finite (298 K) temperature changes in Gibbs free energies (ΔG^0_{298}), fully realizing that our single-electronic-state model cannot ensure a high accuracy for entropy-dependent properties of actinide compounds with their high electronic state densities at rather low energies. One can hope, however, that the changes in entropy at this temperature are not strongly affected by contributions from electronically excited states; the error for vibrorotational contribution to entropy-dependent part of ΔG^0_{298} should be about few kJ/mol and thus less significant than the errors in reaction energies arising from approximate treatment of exchange and correlation effects. Bader net charges of the actinide atoms can be found in Table IV. The agreement between the equilibrium geometry data obtained with the two employed approximations for the exchange-correlation functional is very good; B3LYP bond lengths are slightly but systematically larger (∼0.02 Å) than their PBE0 counterparts while bond angles practically coincide. B3LYP net charges of An atoms are normally less than 1% smaller than PBE0 ones. As for reaction energetics, the differences are non-negligible, and we list both sets of data. It might be worth noting that the ΔH^0_{298} values for the reactions involving PuO_n and Pu_2O_7 differ only slightly from the corresponding electronic energy changes obtained in Ref. 12, i.e., zero-point vibrational plus temperature-dependent contributions are not large.

A. Oxidation state VI

Similarly to PuO_3,[12,30] the AmO_3 molecule has a T-shaped planar equilibrium structure (C_{2v} symmetry). The difference between the shorter (actinyl) and longer Am–O[3] bond lengths in AmO_3 is much more significant than in PuO_3; the two short equivalent Am–O bonds are nearly collinear, so

that one readily identifies the slightly distorted AmO_2 group and a relatively weakly bounded O atom. The Am–O^3 bond is obviously too long for considering it as a double bond, and Am in this case can hardly be identified as hexavalent. The weakening of the longer bond in passing from PuO_3 to AmO_3 also manifests itself energetically (Table III, entry *i*). Two trioxide molecules can form a dimer, An_2O_6, having D_{2h} equilibrium structure with two identical oxygen bridges between actinyl groups. Dissociation enthalpy of Am_2O_6 is smaller than that of Pu_2O_6. The equilibrium structure of the heterooxide molecule $PuAmO_6$ resembles that of An_2O_6 with the obvious symmetry lowering to C_{2v} and its dissociation enthalpy lies somewhat above half the sum of those for homodimers (Table III, entries *iv* and *viii*).

B. Oxidation state VII

A remarkable stability of the plutonium heptoxide molecule has been already pointed out in Ref. 12. The present calculations fully confirm this finding. The equilibrium structure of this molecule (Fig. 1) with all atoms except O^5 and O^6 (the superscript index refers to oxygen atom numbers in Fig. 1) lying in the symmetry plane can be described as two slightly distorted PuO_4 squares with one common oxygen (O^3) vertex. Taking into account the difference of bridge Pu–O bond lengths (Table II), one could discern PuO_4-like and PuO_3-like fragments ($Pu^1O^{1,2,3,4}$ and $Pu^2O^{5,6,7}$); the longest non-bridge bond Pu^2–O^7 corresponds to the longer Pu–O bond in PuO_3. It should be noticed, however, that such interpretation is somewhat artificial since the Bader charges of

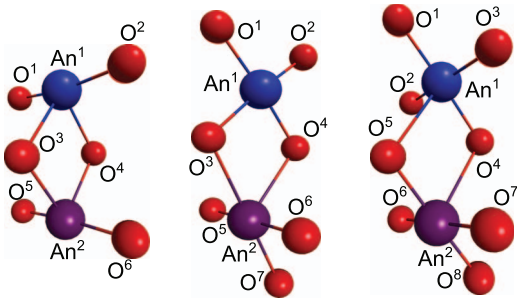

FIG. 1. Equilibrium structures of $An^1An^2O_n$. For heterooxides, An^1=Pu and An^2=Am.

the two Pu atoms nearly coincide while those in free Pu(VIII) and Pu(VI) oxide molecules differ significantly (Table IV). A similar structure is predicted for Am_2O_7; the stability of the latter species is expected to be markedly lower (Table III). One can observe a nearly perfect planarity of the subsystem formed by Am^2 and the neighboring oxygen atoms ($O^{3,5,6,7}$) which is not related to the molecular symmetry (out-of-plane angles are within 1°).

The equilibrium configuration of the mixed heptoxide molecule, $PuAmO_7$, resembles that of Pu_2O_7 and Am_2O_7. It is tempting to identify PuO_4-like and AmO_3-like fragments of this molecule, but the electronic density analysis puts into question the utility of such identification, because the Bader charges of actinide atoms in $PuAmO_7$ are within the same range as those in the corresponding An(VII) oxide molecules, being quite far from the corresponding values for Am(VI) and

TABLE II. Main parameters of equilibrium molecular structures (angles in degrees, distances (r) in Å) according to RDFT/PBE0 calculations (see supplementary material[32]). PuO_n and Pu_2O_7 data from Ref. 12.

		An=Pu	An=Am		Mixed (An^1=Pu, An^2=Am)	
AnO_3	$\angle O^1AnO^2$	170	179			
(C_{2v})	r(An–$O^{1,2}$)	1.75	1.75			
	r(An-O^3)	1.84	2.07			
An_2O_6	$\angle O^1AnO^2$	172	174	$PuAmO_6$	$\angle O^1PuO^2$	171
(D_{2h})	r(An^1–$O^{1,2}$)	1.74	1.73	(C_{2v})	r(Pu–$O^{1,2}$)	1.74
	r(An^1–$O^{3,4}$)	2.08	2.08		r(Pu–$O^{3,4}$)	2.07
					$\angle O^5AmO^6$	175
					r(Am–$O^{5,6}$)	1.72
					r(Am–$O^{3,4}$)	2.08
An_2O_7	r(An^1–O^3)	1.91	1.89	$PuAmO_7$	r(Pu–O^3)	2.21
(C_s)	r(An^2–O^3)	2.20	2.28	(C_s)	r(Am–O^3)	1.95
	r(An^1–O^4)	1.83	1.85		r(Pu–O^4)	1.94
	r(An^2–O^4)	2.39	2.33		r(Am–O^4)	2.32
	r(An^2–O^7)	1.79	2.04		r(Am–O^7)	2.04
	Other r(An–O)	1.74–1.76	1.72–1.77			1.72–1.76
	$\angle An^1O^3An^2$	108	106			106
AnO_4	r(An–O)	1.75	1.74			
(D_{4h})						
An_2O_8	r(An–$O)_{intra}$[a]	1.75–1.83		$PuAmO_8$	r(Pu–$O)_{intra}$	1.75–1.83
(C_{2h})	r(An–$O)_{inter}$[b]	2.42		(C_s)	r(Pu–$O)_{inter}$	2.43
					r(Am–$O)_{intra}$	1.74–1.82
					r(Am–$O)_{inter}$	2.41

[a]Bonds within AnO^4 fragments.
[b]Bonds between the fragments (An^1–O^5, An^2–O^4).

TABLE III. Gas-phase reaction energetics (kJ/mol).

			PBE0	B3LYP	PBE0	B3LYP
			An = Pu		An = Am	
i	$2AnO_3 \rightarrow 2AnO_2 + O_2$	ΔH^0_{298}	252	270	95	108
		ΔG^0_{298}	212	230	58	71
ii	$AnO_4 \rightarrow AnO_2 + O_2$	ΔH^0_{298}	135	147	−7	−24
		ΔG^0_{298}	90	96	−55	−71
iii	$AnO_4 \rightarrow AnO_2(O_2)$	ΔH^0_{298}	−65	−52	−141	−123
		ΔG^0_{298}	−67	−68	−145	−127
iv	$An_2O_6 \rightarrow 2AnO_3$	ΔH^0_{298}	267	276	221	224
		ΔG^0_{298}	208	217	156	160
v	$An_2O_7 \rightarrow AnO_3 + AnO_4$	ΔH^0_{298}	208	202	182	182
		ΔG^0_{298}	153	152	127	126
vi	$An_2O_8 \rightarrow AnO_4 + AnO_4$	ΔH^0_{298}	94	87	90	88
		ΔG^0_{298}	39	42	35	33
			Mixed			
vii	$PuAmO_6 \rightarrow PuO_3 + AmO_3$	ΔH^0_{298}	263	254		
		ΔG^0_{298}	203	194		
viii	$2PuAmO_6 \rightarrow Pu_2O_6 + Am_2O_6$	ΔH^0_{298}	38	8		
		ΔG^0_{298}	41	12		
ix	$PuAmO_7 \rightarrow PuO_4 + AmO_3$	ΔH^0_{298}	197	194		
		ΔG^0_{298}	141	143		
x	$2PuAmO_7 \rightarrow Pu_2O_7 + Am_2O_7$	ΔH^0_{298}	63	54		
		ΔG^0_{298}	63	54		
xi	$PuAmO_8 \rightarrow PuO_4 + AmO_4$	ΔH^0_{298}	92	88		
		ΔG^0_{298}	38	39		
xii	$2PuAmO_8 \rightarrow Pu_2O_8 + Am_2O_8$	ΔH^0_{298}	0	0		
		ΔG^0_{298}	1	−3		

Pu(VIII). The stability of $PuAmO_7$ is somewhat surprising; the changes in enthalpy and Gibbs energy value for the reaction $2PuAmO_7 \rightarrow Pu_2O_7 + Am_2O_7$ are predicted to be about 60 kJ/mol, exceeding the corresponding values for the mixed An(VI) oxide. In principle, one could suppose that the formation of $PuAmO_7$ (and maybe also of $PuAmO_6$) could be related to the appearance of Am in the gas phase along with Pu in the ozonation experiment described in Ref. 9. It should be noticed, however, that high volatility of the mentioned heptoxides similar, e.g., to that of rhenium heptoxide[31] is at least not obvious, so that definitive conclusions cannot be drawn without the information on intermolecular interactions.

C. Oxidation state VIII

Both plutonium tetroxide and americium tetroxide molecules have regular square equilibrium structures (D_{4h} symmetry). Equilibrium An–O distances are close to the An–O bond lengths in actinyl fragments in An(VI) oxides and even slightly shorter than those in AnO_2 molecules (RDFT/PBE0 values 1.80 Å for PuO_2 and 1.81 Å for AmO_2), as it might be expected for octavalent An. It is worth noting that the identification of PuO_4 in Refs. 3 and 4 was based on the supposed similarity of adsorption behavior to tetrahedral OsO_4 and RuO_4 is not well founded because of the essential difference in equilibrium geometries. The square AnO_4 molecules are thermodynamically unstable with respect to the conversion into the corresponding dioxoperoxides, $AnO_2(O_2)$ (Table III, entry *iii*). The latter species, with very short bond between two equatorial oxygen atoms (∼1.31 Å, RDFT/PBE0), correspond to the global minima on the AnO_4 ground-state potential energy surfaces. Formal An oxidation state +6 in dioxoperoxides agrees well with net charge values (Table IV). Americium (VIII) tetroxide molecule should spontaneously decay into dioxide and molecular oxygen at rather low temperatures; Pu(VIII) tetroxide is somewhat more stable (Table III, entry *ii*), but the change in the Gibbs free energy for its decay into PuO_2 and O_2 can become negative for higher temperatures, for instance, those of the experiment described in Refs. 3 and 4 (about 1000 K). It is clear, however, that the possibility to observe An(VIII) oxides should depend on kinetic factors. Both tetroxides can form dimers which are considerably less stable than their counterparts for oxidation states VI and VII; the deformation of AnO_4 squares

TABLE IV. Bader net charges of actinide atoms in oxide molecules derived from RDFT/PBE0 charge densities at equilibrium geometries. The data for PuO_3, PuO_4, and Pu_2O_7 are from Ref. 12.

Oxidation state		An = Pu	An = Am		Pu charge	Am charge
VI	AnO_3	2.52	2.30			
	An_2O_6	2.67	2.53	$PuAmO_6$	2.66	2.54
	$AnO_2(O_2)$	2.44	2.35			
VII	An_2O_7[a]	2.76	2.59	$PuAmO_7$	2.75	2.57
		2.76	2.57			
VIII	AnO_4	2.88	2.72			
	An_2O_8	2.90	2.72	$PuAmO_4$	2.88	2.74

[a]Net charges of An^1 (above) and An^2 (below).

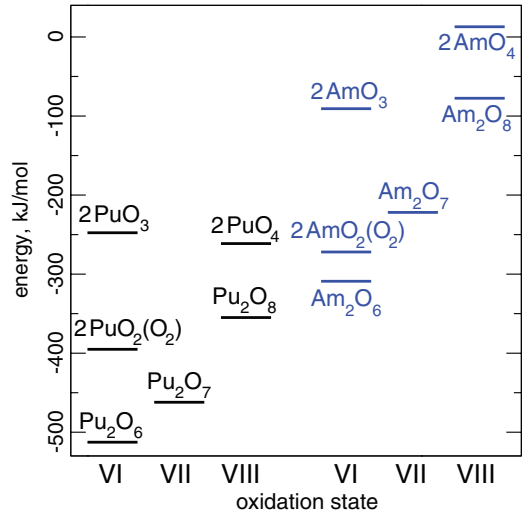

FIG. 2. Energies of $2AnO_{n+2} + (2-n)O_2$ and $An_2O_{n+4} + (2-n/2)O_2$ (0 K, zero-point vibrational energies included) with respect to $2AnO_2 + 2\,O_2$ (RDFT/PBE0).

in the dimers is not strong and the interfragment An–O bonds are much longer than intrafragment ones. The mixed dimer $PuAmO_8$ is nearly isoenergetic with $1/2(Pu_2O_8 + Am_2O_8)$.

Fig. 2 provides a bird's eye view of relative stability of plutonium and americium higher oxides in gas-phase oxides/oxygen system at low temperatures. For both elements, the oxidation states VI and VII appear to be more favorable than VIII; higher oxidation states in oxides are clearly more exotic for Am than for Pu.

IV. CONCLUSIONS

Equilibrium geometries and energetic properties of molecules of higher plutonium and americium oxides are calculated at the DFT level in the frames of accurate small-core two-component relativistic pseudopotential model. The structures of americium oxide molecules closely resemble those of corresponding plutonium oxides, despite the fact that the Am–O bonding is always markedly weaker than Pu–O one. Both actinide atoms in oxidation states VII and VIII tend to be surrounded by four oxygen atoms forming a (distorted) square; the distortions never affect significantly the planarity of AnO_4 subsystems. For both elements, relatively high stability of heptoxide molecules is predicted. The two An atoms in An_2O_7 have structurally non-equivalent positions but bear nearly equal net charges. The mixed hexoxide $PuAmO_6$ and especially heptoxide $PuAmO_7$ molecules are expected to be stable with respect to the transformation into corresponding homooxides Pu_2O_n and Am_2O_n ($n = 6$ or 7). It is possible that the americium volatilization enhancement under ozonation in the presence of Pu is related to the formation of mixed heptoxide or/and hexoxide molecules. Tetroxide structures with formal plutonium or americium oxidation state VIII correspond to local potential energy minima while the global minima is reached at dioxoperoxide structures. The role of peroxides in the chemistry of Pu–oxygen and Am–oxygen systems seems to be very important; a detailed study of these species is now in progress in our group.

ACKNOWLEDGMENTS

We are indebted to Professor C. van Wüllen for supplying us with his relativistic DFT code.[16] Thanks are due to A. A. Granovsky for helpful discussions. The calculations were performed at MCC NRC "Kurchatov Institute" (http://computing.kiae.ru/). The work was supported by the Russian Foundation for Basic Research (Grant Nos. 13-03-01234 and 13-03-01307).

[1] N. N. Krot, A. D. Gelman, F. A. Zakharova, V. F. Peretrukhin, and A. K. Pickaev, Sov. Radiochem. **14**, 922 (1972).
[2] N. N. Krot, A. D. Gelman, M. P. Mefod'eva, V. P. Shilov, V. F. Peretrukhin, and V. I. Spitsyn, *Heptavalent State of Neptunium, Plutonium and Americium, UCRL-Trans-11798* (Lawrence Livermore National Laboratory, Livermore, 1977).
[3] V. P. Domanov, G. V. Buklanov, and Y. V. Lobanov, Radiochemistry **44**, 114 (2002).
[4] V. P. Domanov and Y. V. Lobanov, Radiochemistry **51**, 14 (2009).
[5] S. Hübener, S. Taut, A. Vahle, G. Bernhard, and T. Fanghänel, Radiochim. Acta **96**, 781 (2008).
[6] M. R. Antonio, C. W. Williams, J. A. Sullivan, S. Skanthakumar, Y.-J. Hu, and L. Soderholm, Inorg. Chem. **51**, 5274 (2012).
[7] M. V. Nikonov, Y. M. Kiselev, I. G. Tananaev, and B. F. Myasoedov, Dokl. Chem. **437**, 69 (2011).
[8] B. B. Ebbinghaus, O. H. Krikorian, and M. G. Adamson, ASM 1994 Materials Week, Rosemont, Illinois, USA, 1994 [see also Lawrence Livermore National Laboratory, Report UCRL-JC-116414].
[9] Y. M. Kiselev, M. V. Nikonov, and B. F. Myasoedov, Dokl. Chem. **448**, 12 (2013).
[10] M. Straka, K. G. Dyall, and P. Pyykkö, Theor. Chem. Acc. **106**, 393 (2001).
[11] Y. M. Kiselev, V. M. Nikonov, V. D. Dolzhenko, A. Y. Ermilov, I. G. Tananaev, and B. F. Myasoedov, Dokl Chem. **426**, 91 (2009).
[12] A. V. Zaitsevskii, A. V. Titov, S. S. Malkov, I. G. Tananaev, and Y. M. Kiselev, Dokl. Chem. **448**, 1 (2013).
[13] N. S. Mosyagin, A. N. Petrov, A. V. Titov, and I. I. Tupitsyn, Prog. Theor. Chem. Phys. **B15**, 229 (2006).
[14] N. S. Mosyagin, A. Zaitsevskii, and A. V. Titov, Int. Rev. At. Mol. Phys. **1**, 63 (2010).
[15] A. V. Mitin and C. van Wüllen, J. Chem. Phys. **124**, 064305 (2006).
[16] C. van Wüllen, Z. Phys. Chem. **224**, 413 (2010).
[17] N. S. Mosyagin and A. V. Titov, http://www.qchem.pnpi.spb.ru/recp.
[18] B. O. Roos, R. Lindh, P.-A. Malmqvist, V. Veryazov, and P.-O. Widmark, Chem. Phys. Lett. **409**, 295 (2005).
[19] W. Küchle, M. Dolg, H. Stoll, and H. Preuss, Stuttgart RLC ECP, EMSL basis set library, https://bse.pnl.gov/bse/portal.
[20] K. L. Schuchardt, B. T. Didier, T. Elsethagen, L. Sun, V. Gurumoorthi, J. Chase, J. Li, and T. L. Windus, J. Chem. Inf. Model. **47**, 1045 (2007).
[21] A. Schäfer, C. Huber, and R. Ahlrichs, J. Chem. Phys. **100**, 5829 (1994).
[22] C. Adamo and V. Barone, J. Chem. Phys. **110**, 6158 (1999).
[23] P. J. Stephens, F. J. Devlin, C. F. Chabalowski, and M. J. Frisch, J. Phys. Chem. **98**, 11623 (1994).
[24] B. B. Averkiev, M. Mantina, R. Valero, I. Infante, A. Kovacs, D. G. Truhlar, and L. Gagliardi, Theor. Chem. Acc. **129**, 657 (2011).
[25] A. A. Granovsky, Firefly, version 7.1.G, 2009, http://classic.chem.msu.su/gran/firefly/index.html.
[26] A. Kovacs, P. Pogany, and R. J. M. Koning, Inorg. Chem. **51**, 4841 (2012).
[27] W. Tang, E. Sanville, and G. Henkelman, J. Phys.: Condens. Matter **21**, 084204 (2009).
[28] E. Sanville, S. D. Kenny, R. Smith, and G. Henkelman, J. Comput. Chem. **28**, 899 (2007).
[29] J. Marçalo and J. K. Gibson, J. Phys. Chem. A **113**, 12599 (2009).
[30] B. Schimmelpfennig, T. Privalov, U. Wahlgren, and I. Grenthe, J. Phys. Chem. A **107**, 9705 (2003).
[31] W. T. Smith, L. E. Line, and W. A. Bell, J. Am. Chem. Soc. **74**, 4964 (1952).
[32] See supplementary material at http://dx.doi.org/10.1063/1.4813284 for full equilibrium geometries.